PHILOSOPHICAL TRANSACTIONS A

royalsocietypublishing.org/journal/rsta

Research

Cite this article: Deymier AC, Deymier PA, Latypov M, Muralidharan K. 2023 Effect of stress on the dissolution/crystallization of apatite in aqueous solution: a thermochemical equilibrium study. *Phil. Trans. R. Soc. A* **381**: 20220242.
https://doi.org/10.1098/rsta.2022.0242

Received: 14 August 2022
Accepted: 17 November 2022

One contribution of 13 to a discussion meeting issue 'Supercomputing simulations of advanced materials'.

Subject Areas:
materials science, biophysics, materials science

Keywords:
bone mineralization, thermodynamics, modelling and simulation

Author for correspondence:
Alix C. Deymier
e-mail: deymier@uchc.edu

Effect of stress on the dissolution/crystallization of apatite in aqueous solution: a thermochemical equilibrium study

Alix C. Deymier[1], Pierre A. Deymier[2], Marat Latypov[2,3] and Krishna Muralidharan[2]

[1]Department of Biomedical Engineering, University of Connecticut Health Center, Farmington, CT, USA
[2]Department of Materials Science and Engineering, and [3]Graduate Interdisciplinary Program in Applied Mathematics, University of Arizona, Tucson, AZ 85721, USA

ACD, 0000-0002-1088-7958; KM, 0000-0003-1275-3846

Bone mineralization is critical to maintaining tissue mechanical function. The application of mechanical stress via exercise promotes bone mineralization via cellular mechanotransduction and increased fluid transport through the collagen matrix. However, due to its complex composition and ability to exchange ions with the surrounding body fluids, bone mineral composition and crystallization is also expected to respond to stress. Here, a combination of data from materials simulations, namely density functional theory and molecular dynamics, and experimental studies were input into an equilibrium thermodynamic model of bone apatite under stress in an aqueous solution based on the theory of thermochemical equilibrium of stressed solids. The model indicated that increasing uniaxial stress induced mineral crystallization. This was accompanied by a decrease in calcium and carbonate integration into the apatite solid. These results suggest that weight-bearing exercises can increase tissue mineralization via interactions between bone mineral and body fluid independent of cell and matrix behaviours, thus providing another mechanism by which exercise can improve bone health.

This article is part of a discussion meeting issue 'Supercomputing simulations of advanced materials'.

THE ROYAL SOCIETY PUBLISHING

1. Introduction

Bone is a three phase composite constituted of a proteinaceous collagen matrix, nanocrystalline carbonated apatite and aqueous body fluids [1]. Changes in the relative concentration and organization of these different components cause significant modifications to bone mechanics. For example, decreased mineral content leads to reduced bone modulus resulting in clinical conditions such as rickets and osteomalacia [1–4]. Therefore, it is essential to understand how bone mineralization and mineral content is regulated in the body.

Bone's ability to increase its mineral content and mass in response to mechanical loads, also known as Wolff's Law [5], has been well established with Galileo describing this effect in 1638 [6]. This ability of bone to adapt to the mechanical environment has primarily been attributed to cellular mechanotransduction. Specifically, it has been shown that osteocytes, dendritic cells embedded in the bone matrix, respond to changes in fluid flow through the bone porosity by increasing pro-osteoblastic signalling [7]. These signals recruit and activate bone-depositing osteoblasts resulting in the deposition of greater quantities of more highly mineralized bone tissue. This process has been shown to be in part responsible for the increase in bone density in high-intensity athletes and conversely the bone loss seen in astronauts [8,9].

However, mineralization of bone has also been shown to be physiochemically controlled in the absence of cellular activity. Many studies have shown that the chemistry of the protein matrix enhances the nucleation and growth of bone mineral by reducing the energy barriers to mineralization [10–13]. Further, recent investigations of the effects of fluid shear stress and cyclic loading on collagen matrix mineralization, have shown that increased loading promoted increased matrix mineralization due to improved fluid transport [14,15]. These results suggest that, beyond the chemistry of the matrix, mechanical loading may play a central role in the physiochemical mineralization of bone tissue.

Despite studies of the cellular and matrix mineralization responses to applied loads, little work has been done examining how mechanical forces promote independent crystallization and growth of bone apatite. Bone apatite is a unique calcium phosphate mineral that is highly sensitive to substitutional exchanges in aqueous environments [16]. Specifically, bone apatite contains approximately 6 wt% of carbonate substitutions for phosphate, which is concomitant with an exchange of sodium for calcium to maintain charge balance [16]. These substitutions have been shown to significantly affect the lattice structure, crystal size, solubilty and mechanics of the nanocrystals [17,18]. This complex relationship between substitution, morphology and mechanics has led us to hypothesize that loading may regulate bone mineral dissolution and growth independent of cellular or matrix contributions.

Therefore, in this study we apply a combination of materials simulation, density functional theory (DFT) and molecular dynamics (MD), and experimental data to identifying the consequences of applied load on the dissolution/crystallization of bone apatite in aqueous solutions using the theory of thermochemical equilibrium of solids under stress [19–21]. Our paper is organized as follows. In §2a, we derive the specific conditions for equilibrium between a stressed solid apatite in aqueous solution. Solving these conditions for the equilibrium state requires the knowledge of the equations of states for electrochemical potential of the ionic species in the solid and the solution (§2b). The equilibrium state of the stressed apatite in aqueous solution is referenced to that of the solid/liquid system under hydrostatic pressure (§2c). An approximate solution for the equilibrium state of the solid/liquid system is finally obtained (§2d) by combining literature data from materials simulations and experiments with the linearized theory of thermochemical equilibrium of the stressed solid.

2. Thermochemical equilibrium of solid apatite and water under stress

(a) Conditions for equilibrium

Apatite is a calcium phosphate mineral which can readily substitute sodium (Na^+) for calcium (Ca^{2+}) ions and carbonate (CO_3^{2-}) for phosphate (PO_4^{3-}) ions. This solid is assumed to be in

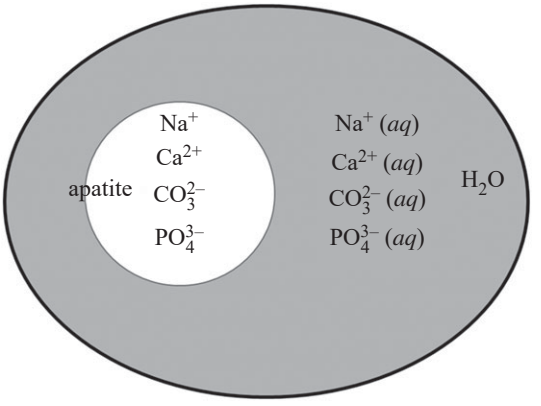

Figure 1. Schematic illustration of the model system. A solid apatite subsystem is separated from an aqueous solution by a boundary that is movable, diathermal and permeable to all ionic chemical species. The outer boundary of the apatite/water composite is rigid, iso-entropic and impermeable to all species.

thermal, mechanical and chemical contact with an aqueous solution of the same constitutive ions (figure 1). We define the following compositional variables for the cationic and anionic species in aqueous solution, C^L_{Na}, C^L_{Ca}, C^L_C, C^L_P. The upper script refers to a liquid solution. We use shorthand notation for the lower indices, Na, Ca, C and P for Na^+, Ca^{2+}, CO_3^{2-} and PO_4^{3-}, respectively. These compositions are defined in terms of number of moles per unit volume of solution. C^L_H also stands for the number of moles of water per unit volume of liquid. The ionic compositions in the solid apatite are defined as C'^S_{Na}, C'^S_{Ca}, C'^S_C, C'^S_P where the upper script S stands for solid. Since the solid may be subjected to mechanical stress (and therefore undergo strain), the prime indicates that the number of moles is taken per unit volume of the solid in the reference state for measuring the strain. All subsequent primed quantities will be per unit volume of reference state for measuring strain. The thermodynamic fundamental equation of this composite system is written in the energy representation as:

$$E = \int_{V'} \mathrm{d}V' e'^S + \int_{V^L} \mathrm{d}V^L e^L, \tag{2.1}$$

where the density of energy per unit volume in the reference state for measuring strain is given by

$$e'^S = e'^S\left(s'^S, \ddot{\varepsilon}, C'^S_{\mathrm{Na}}, C'^S_{\mathrm{Ca}}, C'^S_C, C'^S_P, \boldsymbol{D}^S\right), \tag{2.2}$$

and the density of energy of the liquid solution is

$$e^L = e^L(s^L, C^L_{\mathrm{Na}}, C^L_{\mathrm{Ca}}, C^L_C, C^L_P, C^L_H, \boldsymbol{D}^L). \tag{2.3}$$

In equations (2.2) and (2.3), s'^S and s^L are densities of entropy and $\ddot{\varepsilon}$ is the strain tensor assuming small strain and linear elasticity. $\boldsymbol{D}^S$ and $\boldsymbol{D}^L$ are electric displacement which are functions of the ionic compositions in the solid and liquid, respectively.

The equilibrium state of the apatite/aqueous solution composite system is found by minimizing the total energy (equation (2.1)) with respect to the system's degrees of freedom under

royalsocietypublishing.org/journal/rsta Phil. Trans. R. Soc. A 381: 20220242

constraints. Conservation of number of moles of the different chemical species imposes:

$$\nu_{\mathrm{Na}} = \int_{V'} \mathrm{d}V' C'^{S}_{\mathrm{Na}} + \int_{V^L} \mathrm{d}V^L C^L_{\mathrm{Na}}, \tag{2.4a}$$

$$\nu_{\mathrm{Ca}} = \int_{V'} \mathrm{d}V' C'^{S}_{\mathrm{Ca}} + \int_{V^L} \mathrm{d}V^L C^L_{\mathrm{Ca}}, \tag{2.4b}$$

$$\nu_{C} = \int_{V'} \mathrm{d}V' C'^{S}_{C} + \int_{V^L} \mathrm{d}V^L C^L_{C}, \tag{2.4c}$$

$$\nu_{P} = \int_{V'} \mathrm{d}V' C'^{S}_{P} + \int_{V^L} \mathrm{d}V^L C^L_{P} \tag{2.4d}$$

and

$$\nu_{H} = \int_{V^L} \mathrm{d}V^L C^L_{H}, \tag{2.4e}$$

with ν_{Na}, ν_{Ca}, ν_C, ν_P and ν_H constants.

Charge conservation states that

$$Q = \int_{V'} \mathrm{d}V' e[1C'^{S}_{\mathrm{Na}} + 2C'^{S}_{\mathrm{Ca}} + (-2)C'^{S}_{C} + (-3)C'^{S}_{P}] + \int_{V^L} \mathrm{d}V^L[1C^L_{\mathrm{Na}} + 2C^L_{\mathrm{Ca}} + (-2)C^L_{C} + (-3)C^L_{P}]. \tag{2.5}$$

In equation (2.5), e is the absolute value of the charge of an electron.

Volume conservation associated with mechanical deformation of the solid but also dissolution or recrystallization of the solid apatite is written as

$$(\delta \boldsymbol{u}.\boldsymbol{n}^S)\boldsymbol{n}^S dA + \delta y^S \boldsymbol{n}^S dA = \delta y^L \boldsymbol{n}^L dA. \tag{2.6}$$

In equation (2.6), dA is an element of surface on the solid/liquid interface. We are not using prime quantities for the element of surface of the solid since the solid that may dissolve or recrystallize may do so under stressed (strained) conditions. $\delta \boldsymbol{u}.\boldsymbol{n}^S$ is the normal component of the elastic displacement field $\delta \boldsymbol{u}$, where $\boldsymbol{n}^S$ is the outward normal to the solid/liquid interface. δy^{S} is the amount of dissolution or recrystallization along the solid normal. $\delta y^L \boldsymbol{n}^L dA$ is the change in volume of the liquid due to elastic deformation and dissolution/recrystallization of the solid apatite. Since the normal to the liquid/solid interface $\boldsymbol{n}^L = -\boldsymbol{n}^S$, the volume conservation reduces to

$$\delta y^S + \delta \boldsymbol{u}.\boldsymbol{n}^S = -\delta y^L. \tag{2.7}$$

Entropy conservation imposes that the total entropy be constant, namely:

$$S = \int_{V'} \mathrm{d}V' s'^{S} + \int_{V^L} \mathrm{d}V^L s^L. \tag{2.8}$$

Finally, in the apatite solid, Na^+ and Ca^{2+} substitute for each other on a cation sublattice, such that

$$C'^{S}_{\mathrm{Na}} + C'^{S}_{\mathrm{Ca}} = C'_{+}, \tag{2.9a}$$

where C'_+ is the density of cation sites in the apatite lattice per unit volume of reference state for measuring strain.

In the apatite solid, CO_3^{2-} and PO_4^{3-} substitute for each other on an anion sublattice, such that

$$C'^{S}_{C} + C'^{S}_{P} = C'_{-}, \tag{2.9b}$$

where C'_- is the density of anion sites in the apatite lattice per unit volume of reference state for measuring strain. Following Larché & Cahn [19,20] and Johnson & Schmalzried [21], we employ the Lagrange multipliers method to minimize equation (2.1) with the above constraints. We introduce the Lagrange multipliers μ_{Na}, μ_{Ca}, μ_C, μ_P and μ_H for the constraints given by equations (2.4(*a*–*e*)). We also introduce the multipler θ for entropy conservation (equation (2.8)) and the multiplier ϕ_c for the charge conservation.

royalsocietypublishing.org/journal/rsta Phil. Trans. R. Soc. A 381: 20220242

Variation with respect to the entropy densities leads to the conditions for thermal equilibrium:

$$\frac{\partial e'^S}{\partial s'^S} = \frac{\partial e^L}{\partial s^L} = \theta. \tag{2.10}$$

In equation (2.10), the partial derivatives are taken at constant strain and compositions. Thermal equilibrium is achieved when the temperature is uniform within the solid/liquid composite system.

Again, following [19–21], the variation with respect to geometrical degrees of freedom, namely strain and volume, using the constraint given by equation (2.7), lead to the bulk and interfacial conditions for equilibrium.

Mechanical equilibrium inside the solid requires:

$$\mathrm{div}'\overleftrightarrow{\sigma} = 0, \tag{2.11}$$

where $\overleftrightarrow{\sigma} = \partial e'^S/\partial \overleftrightarrow{\varepsilon}$ is the stress tensor and div′ stands for the divergence expressed in a system of coordinate relative to the reference state for measuring strain.

Mechanical equilibrium at the solid/liquid interface implies that the normal component of the stress at the interface balances the pressure, P, in the liquid:

$$\overleftrightarrow{\sigma}\boldsymbol{n}^S = -P\boldsymbol{n}^S. \tag{2.12}$$

Further, the variation with respect to volume gives the condition for dissolution/recrystallization:

$$j^S = J^L, \tag{2.13a}$$

with

$$\begin{aligned} j^S = e^S - \theta s^S - \phi_c e[1C^S_{\mathrm{Na}} + 2C^S_{\mathrm{Ca}} + (-2)C^S_{\mathrm{C}} + (-3)C^S_P] \\ - \mu_{\mathrm{Na}}C^S_{\mathrm{Na}} - \mu_{\mathrm{Ca}}C^S_{\mathrm{Ca}} - \mu_C C^S_{\mathrm{C}} - \mu_P C^S_P \end{aligned} \tag{2.13b}$$

and

$$\begin{aligned} j^L = e^L - \theta s^L - \phi_c e[1C^L_{\mathrm{Na}} + 2C^L_{\mathrm{Ca}} + (-2)C^L_{\mathrm{C}} + (-3)C^L_P] \\ - \mu_{\mathrm{Na}}C^L_{\mathrm{Na}} - \mu_{\mathrm{Ca}}C^L_{\mathrm{Ca}} - \mu_C C^L_{\mathrm{C}} - \mu_P C^L_P - \mu_H C^L_H, \end{aligned} \tag{2.13c}$$

using Euler's equation for a fluid, $j^L = -P$. Equation (2.13a) simplifies to

$$j^S = -P.$$

This is the condition for dissolution/recrystallization of the solid at the solid/liquid interface. Note that this condition for equilibrium involves unprimed quantities in j^S because the solid that may dissolve or recrystallize may be subjected to stress (or strain). This condition can be converted into densities per unit volume of reference state for measuring strain as follows:

$$j'^S = -P\left(1 + \mathrm{Tr}\overleftrightarrow{\varepsilon}\right). \tag{2.14}$$

Here, $\mathrm{Tr}\overleftrightarrow{\varepsilon}$ stands for the trace of the strain tensor, i.e. the sum of the diagonal terms which effectively represents the relative change in volume due to deformation per unit volume of reference state for measuring strain.

Finally, using the Lagrange multipliers method, the variations with respect to composition in the solid and liquid is obtained as:

$$\int_{V'} \mathrm{d}V' \left\{ \frac{\partial e'^{S}}{\partial C'^{S}_{\mathrm{Na}}}\delta C'^{S}_{\mathrm{Na}} + \frac{\partial e'^{S}}{\partial C'^{S}_{\mathrm{Ca}}}\delta C'^{S}_{\mathrm{Ca}} + \frac{\partial e'^{S}}{\partial C'^{S}_{C}}\delta C'^{S}_{C} + \frac{\partial e'^{S}}{\partial C'^{S}_{P}}\delta C'^{S}_{P} \right.$$
$$- \phi_c e[1\delta C'^{S}_{\mathrm{Na}} + 2\delta C'^{S}_{\mathrm{Ca}} + (-2)\delta C'^{S}_{C} + (-3)\delta C'^{S}_{P}]$$
$$\left. -\mu_{\mathrm{Na}}\delta C'^{S}_{\mathrm{Na}} - \mu_{\mathrm{Ca}}\delta C'^{S}_{\mathrm{Ca}} - \mu_{C}\delta C'^{S}_{C} - \mu_{P}\delta C'^{S}_{P} \right\} + \int_{V'} \mathrm{d}V' \boldsymbol{E}.\delta \boldsymbol{D}^{S}$$
$$+ \int_{V^L} dV^L \left\{ \frac{\partial e^L}{\partial C^L_{\mathrm{Na}}}\delta C^L_{\mathrm{Na}} + \frac{\partial e^L}{\partial C^L_{\mathrm{Ca}}}\delta C^L_{\mathrm{Ca}} + \frac{\partial e^L}{\partial C^L_{C}}\delta C^L_{C} \right.$$
$$+ \frac{\partial e^L}{\partial C^L_{P}}\delta C^L_{P} + \frac{\partial e^L}{\partial C^L_{H}}\delta C^L_{H} \phi_c e[1\delta C^L_{\mathrm{Na}} + 2\delta C^L_{\mathrm{Ca}} + (-2)\delta C^L_{C} + (-3)\delta C^L_{P}]$$
$$\left. - \mu_{\mathrm{Na}}\delta C^L_{\mathrm{Na}} - \mu_{\mathrm{Ca}}\delta C^L_{\mathrm{Ca}} - \mu_{C}\delta C^L_{C} - \mu_{P}\delta C^L_{P} - \mu_{H}\delta C^L_{H} \right\} + \int_{V^L} \mathrm{d}V^L \boldsymbol{E}.\delta \boldsymbol{D}^{L} = 0. \tag{2.15}$$

In equations (2.15), $\boldsymbol{E}$ is the electrostatic field. It is useful to define a scalar potential function, ϕ such that, $\boldsymbol{E} = \nabla\phi$. Using Gauss theorem and the divergence theorem, one can show that

$$\int_{V'} \mathrm{d}V' \boldsymbol{E}.\delta \boldsymbol{D}^{S} = -\int_{A'} \mathrm{d}A' \phi^{S} \delta \boldsymbol{D}^{S} \boldsymbol{n}^{S} + \int_{V'} \mathrm{d}V' \phi^{S} e[1\delta C'^{S}_{\mathrm{Na}} + 2\delta C'^{S}_{\mathrm{Ca}} + (-2)\delta C'^{S}_{C} + (-3)\delta C'^{S}_{P}] \tag{2.16a}$$

and

$$\int_{V^L} \mathrm{d}V^L \boldsymbol{E}.\delta \boldsymbol{D}^{L} = -\int_{A^L} \mathrm{d}A^L \phi^L \delta \boldsymbol{D}^{L} \boldsymbol{n}^{L} + \int_{V^L} \mathrm{d}V^L \phi^L e[1\delta C^L_{\mathrm{Na}} + 2\delta C^L_{\mathrm{Ca}} + (-2)\delta C^L_{C} + (-3)\delta C^L_{P}]. \tag{2.16b}$$

A' and A^{L} are the areas of the solid/liquid interface (effectively the same). ϕ^{S} and ϕ^{L} are the electrostatic potential inside the solid and the liquid regions, respectively.

Inserting equations (2.16*a*,*b*) into equation (2.15) and using $\boldsymbol{n}^L = -\boldsymbol{n}^S$ yields a surface condition for equilibrium stating that the normal components of the electric displacement are equal at the interface:

$$(\delta \boldsymbol{D}^{S} - \delta \boldsymbol{D}^{L})\boldsymbol{n}^{S} = 0. \tag{2.17}$$

By using the lattice constraints (2.9*a*,*b*) reformulated in terms of variations in compositions, namely: $\delta C'^{S}_{\mathrm{Na}} = -\delta C'^{S}_{\mathrm{Ca}}$ and $\delta C'^{S}_{P} = -\delta C'^{S}_{C}$, to eliminate two dependent compositions in the solid, we obtain the conditions for electrochemical chemical equilibrium of the cations by further eliminating the Lagrange multipliers:

$$\eta'^{S}_{\mathrm{Ca}} - \eta'^{S}_{\mathrm{Na}} = \eta^{L}_{\mathrm{Ca}} - \eta^{L}_{\mathrm{Na}}. \tag{2.18}$$

In equation (2.18), we have defined the electrochemical potentials:

$$\eta'^{S}_{\mathrm{Ca}} = \frac{\partial e'^{S}}{\partial C'^{S}_{\mathrm{Ca}}} + \phi^{S} e(2), \tag{2.19a}$$

$$\eta'^{S}_{\mathrm{Na}} = \frac{\partial e'^{S}}{\partial C'^{S}_{\mathrm{Na}}} + \phi^{S} e(1), \tag{2.19b}$$

$$\eta^{L}_{\mathrm{Ca}} = \frac{\partial e^{L}}{\partial C^{L}_{\mathrm{Ca}}} + \phi^{L} e(2) \tag{2.19c}$$

and

$$\eta^{L}_{\mathrm{Na}} = \frac{\partial e^{L}}{\partial C'^{S}_{\mathrm{Na}}} + \phi^{L} e(1). \tag{2.19d}$$

Similarly, we obtain the conditions for electrochemical chemical equilibrium of the anions:

$$\eta'^{S}_{C} - \eta'^{S}_{P} = \eta^{L}_{C} - \eta^{L}_{P}. \tag{2.20}$$

royalsocietypublishing.org/journal/rsta Phil. Trans. R. Soc. A 381: 20220242

In equation (2.18), we have defined the electrochemical potentials:

$$\eta_C'^S = \frac{\partial e'^S}{\partial C_C'^S} + \phi^S e(-2), \tag{2.21a}$$

$$\eta_P'^S = \frac{\partial e'^S}{\partial C_P'^S} + \phi^S e(-3), \tag{2.21b}$$

$$\eta_C^L = \frac{\partial e^L}{\partial C_C^L} + \phi^L e(-2) \tag{2.21c}$$

and

$$\eta_P^L = \frac{\partial e^L}{\partial C_P'^S} + \phi^L e(-3). \tag{2.21d}$$

The quantities, $\eta_{Ca}'^S - \eta_{Na}'^S = M_{Ca,Na}$ and $\eta_C'^S - \eta_P'^S = M_{C,P}$ are electrochemical diffusion potential. These quantities state, for instance, that change in the electrochemical potential of calcium ions is accompanied by a change in electrochemical potential of sodium ions because of the cation sublattice constraint. A similar statement is made about the anion sublattice constraint.

(b) Equations of state

Following [19–21], the equation of state giving the cation electrochemical diffusion potential as a function of stress and independent composition, $C_{Ca}'^S$ can be expressed relative to the hydrostatic case as:

$$M_{Ca,Na}\left(\overleftrightarrow{\sigma}, C_{Ca}'^S\right) = M_{Ca,Na}(-P\delta_{ij}, C_{Ca}'^S) - \xi_{ij}\delta_{ij}(\sigma_{ij} + P\delta_{ij}) - \frac{1}{2}\frac{\partial S_{ijkl}}{\partial C_{Ca}'^S}\sigma_{kl}\sigma_{ij} + \frac{1}{2}P^2\frac{\partial S_{ijkl}}{\partial C_{Ca}'^S}\delta_{kl}\delta_{ij}, \tag{2.22}$$

where $-P\delta_{ij}$ is the hydrostatic stress (δ_{ij} is the Kroenecker symbol). ξ_{ij} is the chemical expansion coefficient relating the chemical strain (expansion or contraction of the solid) to changes in the independent composition $C_{Ca}'^S$. $\partial S_{ijkl}/\partial C_{Ca}'^S$ is the change in the components of the compliance tensor, S_{ijkl}, of the solid with changes in independent composition $C_{Ca}'^S$. A similar equation of state can be derived for the anion electrochemical diffusion potential:

$$M_{C,P}\left(\overleftrightarrow{\sigma}, C_C'^S\right) = M_{C,P}(-P\delta_{ij}, C_C'^S) - \zeta_{ij}\delta_{ij}(\sigma_{ij} + P\delta_{ij}) - \frac{1}{2}\frac{\partial S_{ijkl}}{\partial C_C'^S}\sigma_{kl}\sigma_{ij} + \frac{1}{2}P^2\frac{\partial S_{ijkl}}{\partial C_C'^S}\delta_{kl}\delta_{ij}. \tag{2.23}$$

In equation (23), the chemical expansion coefficient for the anionic species is ζ_{ij}. In equations (2.22) and (2.23), we have used Einstein notation for summation over repeating indices.

We now assume simple ideal solid solutions for the cations and anions under hydrostatic pressure such that

$$\begin{aligned} M_{Ca,Na}(-P\delta_{ij}, C_{Ca}'^S) = \eta_{Ca}'^S(-P\delta_{ij}, C_{Ca}'^S) - \eta_{Na}'^S(-P\delta_{ij}, C_{Na}'^S) = \mu_{Ca}^0 + R\theta \ln C_{Ca}'^S \\ + \phi^S e(2) - (\mu_{Na}^0 + R\theta \ln C_{Na}'^S + \phi^S e(1)) \end{aligned} \tag{2.24a}$$

and

$$\begin{aligned} M_{C,P}(-P\delta_{ij}, C_C'^S) = \eta_C'^S(-P\delta_{ij}, C_C'^S) - \eta_P'^S(-P\delta_{ij}, C_P'^S) = \mu_C^0 + R\theta \ln C_C'^S \\ + \phi^S e(-2) - (\mu_P^0 + R\theta \ln C_P'^S + \phi^S e(-3)). \end{aligned} \tag{2.24b}$$

In equations (2.24*a*,*b*), μ_{Ca}^0, μ_{Na}^0, μ_C^0 and μ_P^0 are chemical potentials of the ionic species in some standard state under hydrostatic pressure. R is the ideal gas constant. We also recall the sublattice constraints in equations (2.9*a*,*b*).

Similarly, we assume ideal solution behaviour for the liquid such that

$$\eta_{Ca}^L - \eta_{Na}^L = \mu_{Ca}^{0L} + R\theta \ln C_{Ca}^L + \phi^L e(2) - (\mu_{Na}^{0L} + R\theta \ln C_{Na}^L + \phi^L e(1)) \tag{2.25a}$$

and

$$\eta_C^L - \eta_P^L = \mu_C^{0L} + R\theta \ln C_C^L + \phi^L e(-2) - (\mu_P^{0L} + R\theta \ln C_P^L + \phi^L e(-3)). \tag{2.25b}$$

(c) Using hydrostatic pressure as reference

Under hydrostatic stress the conditions for equilibrium (equations (2.18) and (2.20)) are rewritten

$$\bar{\eta}'^{S}_{\mathrm{Ca}} - \bar{\eta}'^{S}_{\mathrm{Na}} = \bar{\eta}^{L}_{\mathrm{Ca}} - \bar{\eta}^{L}_{\mathrm{Na}} \tag{2.26}$$

and

$$\bar{\eta}'^{S}_{C} - \bar{\eta}'^{S}_{P} = \bar{\eta}^{L}_{C} - \bar{\eta}^{L}_{P}. \tag{2.27}$$

In all subsequent equations, we use a bar as an accent above thermodynamic quantities under hydrostatic pressure. Taking the difference between equations (2.18) and (2.26) as well as between equations (2.20) and (2.27), and using the equations of state presented in §2b, we obtain the conditions:

$$R\theta \ln \frac{C'^{S}_{\mathrm{Ca}}}{\bar{C}'^{S}_{\mathrm{Ca}}} \frac{\bar{C}'^{S}_{\mathrm{Na}}}{C'^{S}_{\mathrm{Na}}} + (\phi^{S} - \bar{\phi}^{S}) e((2) - (1)) - \xi_{ij}\delta_{ij}(\sigma_{ij} + P\delta_{ij}) - \frac{1}{2}\frac{\delta S_{ijkl}}{\delta C'^{S}_{\mathrm{Ca}}}\sigma_{kl}\sigma_{ij}$$
$$+ \frac{1}{2}P^{2}\frac{\delta S_{ijkl}}{\delta C'^{S}_{\mathrm{Ca}}}\delta_{kl}\delta_{ij} = R\theta \ln \frac{C^{L}_{\mathrm{Ca}}}{\bar{C}^{L}_{\mathrm{Ca}}} \frac{\bar{C}^{S}_{\mathrm{Na}}}{C^{L}_{\mathrm{Na}}} + (\phi^{L} - \bar{\phi}^{L}) e((2) - (1)) \tag{2.28a}$$

and

$$R\theta \ln \frac{C'^{S}_{\mathrm{C}}}{\bar{C}'^{S}_{\mathrm{C}}} \frac{\bar{C}'^{S}_{\mathrm{P}}}{C'^{S}_{\mathrm{P}}} + (\phi^{S} - \bar{\phi}^{S}) e((-2) - (-3)) - \xi_{ij}\delta_{ij}(\sigma_{ij} + P\delta_{ij}) - \frac{1}{2}\frac{\delta S_{ijkl}}{\delta C'^{S}_{\mathrm{C}}}\sigma_{kl}\sigma_{ij}$$
$$+ \frac{1}{2}P^{2}\frac{\delta S_{ijkl}}{\delta C'^{S}_{\mathrm{C}}}\delta_{kl}\delta_{ij} = R\theta \ln \frac{C^{L}_{\mathrm{C}}}{\bar{C}^{L}_{\mathrm{C}}} \frac{\bar{C}^{L}_{\mathrm{P}}}{C^{L}_{\mathrm{P}}} + (\phi^{L} - \bar{\phi}^{L}) e((-2) - (-3)). \tag{2.28b}$$

The condition for equilibrium with respect to dissolution/recrystallization (equation (2.14)):

$$j'^{S} = e'^{S} - \theta s'^{S} - \phi_{c} e[1C'^{S}_{\mathrm{Na}} + 2C'^{S}_{\mathrm{Ca}} + (-2)C'^{S}_{C} + (-3)C'^{S}_{P}]$$
$$- \mu_{\mathrm{Na}}C'^{S}_{\mathrm{Na}} - \mu_{\mathrm{Ca}}C'^{S}_{\mathrm{Ca}} - \mu_{C}C'^{S}_{C} - \mu_{P}C'^{S}_{P} = -P\left(1 + \mathrm{Tr}\overleftrightarrow{\varepsilon}\right),$$

can be reformulated by eliminating the Lagrange multipliers as was done in §2*a* such that:

$$j'^{S} = f'^{S} - \eta^{L}_{\mathrm{Na}}C'^{S}_{\mathrm{Na}} - \eta^{L}_{\mathrm{Ca}}C'^{S}_{\mathrm{Ca}} - \eta^{L}_{C}C'^{S}_{C} - \eta^{L}_{P}C'^{S}_{P} = -P\left(1 + \mathrm{Tr}\overleftrightarrow{\varepsilon}\right). \tag{2.29}$$

Here, we have defined the density of Helmholtz free energy $f'^{S} = e'^{S} - \theta s'^{S}$. Under hydrostatic pressure, equation (2.29) takes the form:

$$\bar{j}'^{S} = \bar{f}'^{S} - \bar{\eta}^{L}_{\mathrm{Na}}\bar{C}'^{S}_{\mathrm{Na}} - \bar{\eta}^{L}_{\mathrm{Ca}}\bar{C}'^{S}_{E} - \bar{\eta}^{L}_{C}\bar{C}'^{S}_{C} - \bar{\eta}^{L}_{P}\bar{C}'^{S}_{P} = -P(1 + \mathrm{Tr}\overleftrightarrow{\bar{\varepsilon}}). \tag{2.30}$$

Taking the difference between equations (2.29) and (2.30), using the sublattice constraints and the equations of states from §2b, yields, after a number of algebraic manipulations:

$$[f'^{S} - \eta'^{S}_{\mathrm{Ca}}(-P\delta_{ij}, C'^{S}_{\mathrm{Ca}})C'^{S}_{\mathrm{Ca}} - \eta'^{S}_{\mathrm{Na}}(-P\delta_{ij}, C'^{S}_{\mathrm{Ca}})C'^{S}_{\mathrm{Na}} - \eta'^{S}_{C}(-P\delta_{ij}, C'^{S}_{C})C'^{S}_{C}$$
$$-\eta'^{S}_{P}(-P\delta_{ij}, C'^{S}_{C})C'^{S}_{P}] - [\bar{f}'^{S} - \bar{\eta}'^{S}_{\mathrm{Ca}}(-P\delta_{ij}, \bar{C}'^{S}_{\mathrm{Ca}})\bar{C}'^{S}_{\mathrm{Ca}} - \bar{\eta}'^{S}_{\mathrm{Na}}(-P\delta_{ij}, \bar{C}'^{S}_{\mathrm{Ca}})\bar{C}'^{S}_{\mathrm{Na}}$$
$$-\bar{\eta}'^{S}_{C}(-P\delta_{ij}, \bar{C}'^{S}_{C})\bar{C}'^{S}_{C} - \bar{\eta}'^{S}_{P}(-P\delta_{ij}, \bar{C}'^{S}_{C})\bar{C}'^{S}_{P}] + P\left(\mathrm{Tr}\overleftrightarrow{\varepsilon} - \mathrm{Tr}\overleftrightarrow{\bar{\varepsilon}}\right)$$
$$= \left[-\xi_{ij}\delta_{ij}(\sigma_{ij} + P\delta_{ij}) - \frac{1}{2}\frac{\partial S_{ijkl}}{\partial C'^{S}_{\mathrm{Ca}}}\sigma_{kl}\sigma_{ij} + \frac{1}{2}P^{2}\frac{\partial S_{ijkl}}{\partial C'^{S}_{\mathrm{Ca}}}\delta_{kl}\delta_{ij}\right]C'^{S}_{\mathrm{Ca}}$$
$$+ \left[-\zeta_{ij}\delta_{ij}(\sigma_{ij} + P\delta_{ij}) - \frac{1}{2}\frac{\partial S_{ijkl}}{\partial C'^{S}_{C}}\sigma_{kl}\sigma_{ij} + \frac{1}{2}P^{2}\frac{\partial S_{ijkl}}{\partial C'^{S}_{C}}\delta_{kl}\delta_{ij}\right]C'^{S}_{C}$$
$$+ C'_{+}[\eta^{L}_{\mathrm{Na}} - \bar{\eta}^{L}_{\mathrm{Na}} - (\eta'^{S}_{\mathrm{Na}}(-P\delta_{ij}, C'^{S}_{\mathrm{Ca}}) - \bar{\eta}'^{S}_{\mathrm{Na}}(-P\delta_{ij}, \bar{C}'^{S}_{\mathrm{Ca}}))]$$
$$+ C'_{-}[\eta^{L}_{P} - \bar{\eta}^{L}_{P} - (\eta'^{S}_{P}(-P\delta_{ij}, C'^{S}_{C}) - \bar{\eta}'^{S}_{P}(-P\delta_{ij}, \bar{C}'^{S}_{C}))]. \tag{2.31}$$

The difference between the square brackets on the right-hand side of equation (2.31) is effectively the difference in elastic energy of the stressed and hydrostatic solid. In linear elasticity and for an isotropic solid, it is equal to $-\nu/2Y\left(\mathrm{Tr}\vec{\vec{\sigma}}\right)^2 + (1+\nu/2Y)\sigma_{ij}\sigma_{ij} - (3(1-2\nu)/2Y)P^2$, where ν and Y are Poisson's ratio and Young's modulus. Note that this elastic energy is a density per unit volume of the reference state for measuring strain. If the apatite solid considered here is a polycrystalline aggregate, then the assumption of isotropic behaviour is justified. The quantity $P\left(\mathrm{Tr}\vec{\vec{\varepsilon}} - \mathrm{Tr}\overleftrightarrow{\vec{\varepsilon}}\right)$ is the density of work done by the liquid on the solid as it deforms, it is given by: $(1-2\nu/Y)P\mathrm{Tr}\vec{\vec{\sigma}} + (3(1-2\nu)/Y)P^2$.

Using the ideal solution equations of state, the last two terms of equation (2.31) reduce to $C'_+[R\theta\ln(\,C^L_{\mathrm{Na}}/\bar{C}^L_{\mathrm{Na}})\,(\,\bar{C}'^S_{\mathrm{Na}}/C'^S_{\mathrm{Na}}) + ((\phi^L-\bar{\phi}^L)-(\phi^S-\bar{\phi}^S))e(1)] + C'_-[R\theta\ln(\,C^L_P/\bar{C}^L_P)\,(\,\bar{C}'^S_P/C'^S_P) + ((\phi^L-\bar{\phi}^L)-(\phi^S-\bar{\phi}^S))e(-3)]$. Imposing the continuity of the electrostatic potential across the solid/liquid interface such that the electric field does not diverge at that interface, eliminates the second term in each square bracket. The condition for dissolution/recrystallization simplifies to:

$$\begin{aligned}
&-\frac{\nu}{2Y}\left(\mathrm{Tr}\vec{\vec{\sigma}}\right)^2 + \frac{1+\nu}{2Y}\sigma_{ij}\sigma_{ij} - \frac{3(1-2\nu)}{2Y}P^2 + \frac{1-2\nu}{Y}P\mathrm{Tr}\vec{\vec{\sigma}} + \frac{3(1-2\nu)}{Y}P^2 \\
&= \left[-\xi_{ij}\delta_{ij}(\sigma_{ij}+P\delta_{ij}) - \frac{1}{2}\frac{\partial S_{ijkl}}{\partial C'^S_{\mathrm{Ca}}}\sigma_{kl}\sigma_{ij} + \frac{1}{2}P^2\frac{\partial S_{ijkl}}{\partial C'^S_{\mathrm{Ca}}}\delta_{kl}\delta_{ij}\right]C'^S_{\mathrm{Ca}} \\
&\quad + \left[-\zeta_{ij}\delta_{ij}(\sigma_{ij}+P\delta_{ij}) - \frac{1}{2}\frac{\partial S_{ijkl}}{\partial C'^S_{\mathrm{C}}}\sigma_{kl}\sigma_{ij} + \frac{1}{2}P^2\frac{\partial S_{ijkl}}{\partial C'^S_{\mathrm{C}}}\delta_{kl}\delta_{ij}\right]C'^S_{\mathrm{C}} \\
&\quad + C'_+R\theta\ln\frac{C^L_{\mathrm{Na}}}{\bar{C}^L_{\mathrm{Na}}}\frac{\bar{C}'^S_{\mathrm{Na}}}{C'^S_{\mathrm{Na}}} + C'_-R\theta\ln\frac{C^L_P}{\bar{C}^L_P}\frac{\bar{C}'^S_P}{C'^S_P}.
\end{aligned} \tag{2.32}$$

Recall that this condition is applied to the interface region between the solid and the liquid.

(d) Finding the equilibrium state

The ultimate problem in finding the equilibrium state of the apatite/water composite system is to solve equations (2.28*a*,*b*) and (2.32) simultaneously with the constraints of conservation of species and charge conservation as well as Poisson's equations relating electrostatic potentials in the solid and fluid to compositions (charges). We can simplify this complex problem by assuming that the equilibrium compositions in the solid and liquid are uniform in their respective regions. That is, we assume that there is no formation of a space charge distribution at the solid/liquid interface. This assumption allows us to focus on solving for the equilibrium compositions at the solid/liquid interface (which will be the same as the bulk composition). At the interface we have seen that $\phi^{\mathrm{L}} = \phi^{\mathrm{S}}$ and $\bar{\phi}^L = \bar{\phi}^S$. This enables us to simplify equations (2.28*a*,*b*) by eliminating the terms involving the electrostatic potentials. The problem at hand reduces to solving equation (2.32) with the reduced equations:

$$R\theta\ln\frac{C'^S_{\mathrm{Ca}}}{\bar{C}'^S_{\mathrm{Ca}}}\frac{\bar{C}'^S_{\mathrm{Na}}}{C'^S_{\mathrm{Na}}} - \xi_{ij}\delta_{ij}(\sigma_{ij}+P\delta_{ij}) - \frac{1}{2}\frac{\partial S_{ijkl}}{\partial C'^S_{\mathrm{Ca}}}\sigma_{kl}\sigma_{ij} + \frac{1}{2}P^2\frac{\partial S_{ijkl}}{\partial C'^S_{\mathrm{Ca}}}\delta_{kl}\delta_{ij} = R\theta\ln\frac{C^L_{\mathrm{Ca}}}{\bar{C}^L_{\mathrm{Ca}}}\frac{\bar{C}^L_{\mathrm{Na}}}{C^L_{\mathrm{Na}}} \tag{2.33a}$$

and

$$R\theta\ln\frac{C'^S_{\mathrm{C}}}{\bar{C}'^S_{\mathrm{C}}}\frac{\bar{C}'^S_P}{C'^S_P} - \zeta_{ij}\delta_{ij}(\sigma_{ij}+P\delta_{ij}) - \frac{1}{2}\frac{\partial S_{ijkl}}{\partial C'^S_{\mathrm{C}}}\sigma_{kl}\sigma_{ij} + \frac{1}{2}P^2\frac{\partial S_{ijkl}}{\partial C'^S_{\mathrm{C}}}\delta_{kl}\delta_{ij} = R\theta\ln\frac{C^L_{\mathrm{C}}}{\bar{C}^L_{\mathrm{C}}}\frac{\bar{C}^L_P}{C^L_P}. \tag{2.33b}$$

We linearize these equations by writing:

$$C'^S_{\mathrm{Ca}} = \bar{C}'^S_{\mathrm{Ca}} + \Delta'_{\mathrm{Ca}}, \tag{2.34a}$$

$$C'^S_{\mathrm{Na}} = \bar{C}'^S_{\mathrm{Na}} - \Delta'_{\mathrm{Ca}}, \tag{2.34b}$$

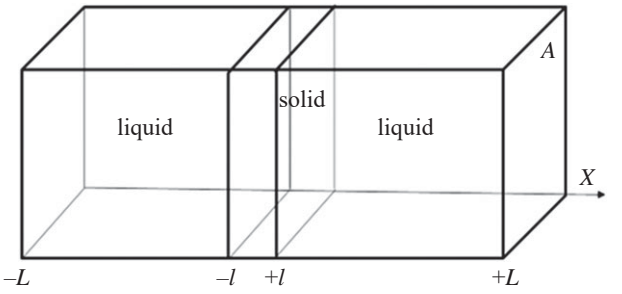

Figure 2. Schematic illustration of geometry of the model solid/liquid composite system. Periodic boundary conditions are imposed in the direction *X* such that the system is effectively a torus. The area of the cross section of the torus is A. All external boundaries are rigid.

$$C_C'^S = \bar{C}_C'^S + \Delta_C' \tag{2.34c}$$

and

$$C_P'^S = \bar{C}_P'^S - \Delta_C', \tag{2.34d}$$

Δ_{Ca}' and Δ_C' are the change in cation and anion compositions due to stress from the compositions under hydrostatic conditions. In the limit of small variations in compositions, we linearize the logarithms using Taylor expansions to first order:

$$\ln \frac{C_{Ca}'^S}{\bar{C}_{Ca}'^S} \frac{\bar{C}_{Na}'^S}{C_{Na}'^S} \tilde{\Delta}_{Ca}' \left(\frac{1}{\bar{C}_{Ca}'^S} + \frac{1}{\bar{C}_{Na}'^S} \right) \tag{2.35a}$$

and

$$\ln \frac{C_C'^S}{\bar{C}_C'^S} \frac{\bar{C}_P'^S}{C_P'^S} \tilde{\Delta}_{Ca}' \left(\frac{1}{\bar{C}_C'^S} + \frac{1}{\bar{C}_P'^S} \right). \tag{2.35b}$$

We now define the geometry of the solid/liquid composite in order to linearize the logarithms on the right-hand sides of equation (2.33*a*,*b*). Figure 2 illustrates the geometry of the composite system.

The conservation of the number of moles of sodium ions under the assumption of uniform compositions in the liquid and solid given by equation (2.4*a*) reduces to

$$\upsilon_{Na} = 2l' A C_{Na}'^S + 2(L - l) A C_{Na}^L,$$

where L and l are defined in figure 2.

Changing the solid units to quantities per unit volume of reference state for measuring strain gives:

$$\upsilon_{Na} = 2lA C_{Na}^S + 2(L - l) A C_{Na}^L.$$

We therefore have:

$$\frac{\upsilon_{Na} - 2lA C_{Na}^S}{2(L - l)A} = C_{Na}^L. \tag{2.36a}$$

Similarly, under hydrostatic pressure, we have

$$\frac{\upsilon_{Na} - 2\bar{l}A \bar{C}_{Na}^S}{2(L - \bar{l})A} = \bar{C}_{Na}^L. \tag{2.36b}$$

We can obtain equivalent expressions for the calcium ion:

$$\frac{\upsilon_{Ca} - 2lA C_{Ca}^S}{2(L - l)A} = C_{Ca}^L \tag{2.37a}$$

and

$$\frac{\upsilon_{Ca} - 2\bar{l}A \bar{C}_{Ca}^S}{2(L - \bar{l})A} = \bar{C}_{Ca}^L. \tag{2.37b}$$

Recognizing that $2\bar{l}A = \bar{V}^S$ and $2(L-\bar{l})A = \bar{V}^L$, defining $l = \bar{l} + \Delta l$, and converting the quantities per unit volume of stressed states into quantities per unit volume of reference state for measuring strain through the multiplicative factor C'_+/C_+, we can approximate to first order:

$$\ln \frac{C^L_{Ca}}{\bar{C}^L_{Ca}} \frac{\bar{C}^L_{Na}}{C^L_E} \sim -2\frac{\Delta l A}{\bar{V}^L}\left[\frac{\bar{C}^S_{Ca}}{\bar{C}^L_{Ca}} - \frac{\bar{C}^S_{Na}}{\bar{C}^L_{Na}}\right] - \frac{\bar{V}^S}{\bar{V}^L}\frac{C_+}{C'_+}\Delta'_{Ca}\left[\frac{1}{\bar{C}^L_{Ca}} + \frac{1}{\bar{C}^L_{Na}}\right]. \tag{2.38}$$

Combining equation (2.38) and (2.35*a*) into equation (2.33*a*) yields:

$$\Delta'_{Ca}\left(\frac{1}{\bar{C}'^S_{Ca}} + \frac{1}{\bar{C}'^S_{Na}} + F\frac{C_+}{C'_+}\left[\frac{1}{\bar{C}^L_{Ca}} + \frac{1}{\bar{C}^L_{Na}}\right]\right) + \frac{X}{R\theta} = -\frac{\Delta l}{L-\bar{l}}\left[\frac{\bar{C}^S_{Ca}}{\bar{C}^L_{Ca}} - \frac{\bar{C}^S_{Na}}{\bar{C}^L_{Na}}\right], \tag{2.39a}$$

where $X = -\xi_{ij}\delta_{ij}(\sigma_{ij} + P\delta_{ij}) - 1/2(\partial S_{ijkl}/\partial C'^S_{Ca})\sigma_{kl}\sigma_{ij} + 1/2P^2(\partial S_{ijkl}/\partial C'^S_{Ca})\delta_{kl}\delta_{ij}$ and $\bar{V}^S/\bar{V}^L = F$. We have also used $1/L - \bar{l} = 2A/\bar{V}^L$.

Similarly to the cationic condition for equilibrium, equation (2.33*b*) can be approximated by:

$$\Delta'_{C}\left(\frac{1}{\bar{C}'^S_{C}} + \frac{1}{\bar{C}'^S_{P}} + F\frac{C_-}{C'_-}\left[\frac{1}{\bar{C}^L_{C}} + \frac{1}{\bar{C}^L_{P}}\right]\right) + \frac{Z}{R\theta} = -\frac{\Delta l}{L-\bar{l}}\left[\frac{\bar{C}^S_{C}}{\bar{C}^L_{C}} - \frac{\bar{C}^S_{P}}{\bar{C}^L_{P}}\right], \tag{2.39b}$$

where $Z = -\zeta_{ij}\delta_{ij}(\sigma_{ij} + P\delta_{ij}) - 1/2(\partial S_{ijkl}/\partial C'^S_{C})\sigma_{kl}\sigma_{ij} + 1/2P^2(\partial S_{ijkl}/\partial C'^S_{C})\delta_{kl}\delta_{ij}$.

The condition for dissolution/recrystallization (equation (2.32)) is also approximated by:

$$\begin{aligned}\mathcal{E} - X\bar{C}'^S_{Ca} - Z\bar{C}'^S_{C} = &\left[X + C'_+R\theta\frac{1}{\bar{C}'^S_{Na}}\left(1 + F\frac{C_+}{C'_+}\frac{\bar{C}'^S_{Na}}{\bar{C}^L_{Na}}\right)\right]\Delta'_{Ca}\\ &+\left[Z + C'_-R\theta\frac{1}{\bar{C}'^S_{P}}\left(1 + F\frac{C_-}{C'_-}\frac{\bar{C}'^S_{P}}{\bar{C}^L_{P}}\right)\right]\Delta'_{C}\\ &+\frac{\Delta L}{L-\bar{l}}R\theta\left[C'_+\left(1 - \frac{\bar{C}^S_{Na}}{\bar{C}^L_{Na}}\right) + C'_-\left(1 - \frac{\bar{C}^S_{P}}{\bar{C}^L_{P}}\right)\right],\end{aligned} \tag{2.39c}$$

where $\mathcal{E} = -(\nu/2Y)\left(\mathrm{Tr}\vec{\vec{\sigma}}\right)^2 + (1+\nu/2Y)\sigma_{ij}\sigma_{ij} - (3(1-2\nu)/2Y)P^2 + (1-2\nu/Y)P\mathrm{Tr}\vec{\vec{\sigma}} + (3(1-2\nu)/Y)P^2$.

The linearized set of equations (2.39*a*,*b*,*c*) can now be further simplified by introducing the partition coefficients under hydrostatic pressure: $k_{Ca} = \bar{C}^S_{Ca}/\bar{C}^L_{Ca}$, $k_{Na} = \bar{C}^S_{Na}/\bar{C}^L_{Na}$, $k_C = \bar{C}^S_C/\bar{C}^L_C$ and $k_P = \bar{C}^S_P/\bar{C}^L_P$. We now have three equations and three unknowns: Δ'_{Ca}, Δ'_C and Δl.

(e) Approximate solution

In this section, we use previously obtained experimental and computational data to solve numerically for the equilibrium state of a solid apatite under stress with the aqueous solution. First of all, we anticipate that the effect of substitution of Ca^{2+} by Na^+ on the chemical expansion and the elastic properties of the apatite will be significantly smaller than the effect of exchange between the larger anions CO_3^{2-} and PO_4^{3-}. This allows us to neglect the term X in the conditions for equilibrium. Furthermore, comparing lattice structures of apatites synthesized with varying amounts of CO_3^{2-}, we have previously shown that a 15 wt% change of CO_3^{2-} content in apatite increases the c-axis and decreases the a-axis lattice spacing by less than 1.1% using X-ray diffraction [17]. It allows us, for an apatite aggregate, to neglect the term involving the chemical expansion coefficient ζ_{ij} in the quantity Z. Therefore, $Z \tilde{-} (1/2)(\partial S_{ijkl}/\partial C'^S_C)\sigma_{kl}\sigma_{ij} + 1/2P^2(\partial S_{ijkl}/\partial C'^S_C)\delta_{kl}\delta_{ij}$. To obtain information about the mineral mechanics as a function of composition, we turn to literature studies using both computational and experimental approaches. Using previously established parameters for stoichiometric hydroxyapatite [22–24], models for carbonate substituted apatite have been developed via the gradual increase of CO_3^{2-} substitutions for PO_4^{3-} in the structure [17,25]. Elastic constants have then been calculated by fitting Hooke's Law for both stress–strain (Molecular Static) and energy-strain (DFT) relations

for infinitesimal deformations [17,26–28]. Our study using these techniques to predict the effect of CO_3^{2-} on the compliance of apatites showed that the addition of CO_3^{2-} to the lattice can decrease the elastic moduli by nearly 50% [17]. These results were experimentally confirmed using high-energy synchrotron X-ray diffraction in combination with applied fluid-mediated hydrostatic loading showing a decrease in modulus from 127 GPa to 57 GPa [18]. Therefore, $Z \sim -\frac{1}{2}\frac{\partial S_{ijkl}}{\partial C_C^S}\sigma_{kl}\sigma_{ij} + \frac{1}{2}P^2\frac{\partial S_{ijkl}}{\partial C_C^S}\delta_{kl}\delta_{ij}$. Finally, under our previous assumption of an isotropic solid, we consider the application of a non-hydrostatic stress $\vec{\sigma}$ whose components are all zero but $\sigma_{11} = \sigma$ where $\sigma \gg P$. Neglecting the hydrostatic pressure terms, we obtain $\mathcal{E} \sim \sigma^2/2Y$. Under the same approximation, $Z \sim -(1/Y)(\partial Y/\partial C_C'^S)\mathcal{E}$.

Equation (2.39*a*) becomes:

$$\Delta'_{Ca} \tilde{-} \frac{\Delta l}{L - \bar{l}} \frac{[k_{Ca} - k_{Na}]}{R_1}, \tag{2.40a}$$

where $R_1 = (1/\bar{C}_{Ca}'^S + 1/\bar{C}_{Na}'^S + F(C_+/C')[1/\bar{C}_{Ca}^L + 1/\bar{C}_{Na}^L]) > 0$.

Equation (2.39*b*) takes the form:

$$\Delta'_C = \left(-\frac{Z}{R\theta} - \frac{\Delta l}{L - \bar{l}}[k_C - k_P]\right)/R_2, \tag{2.40b}$$

where $R_2 = (1/\bar{C}_C'^S + 1/\bar{C}_P'^S + F(C_-/C'_-)[1/\bar{C}_C^L + 1/\bar{C}_P^L]) > 0$.

By inserting equations (2.40*a*,*b*) into equation (2.39*c*), we can solve for $\Delta l/L - \bar{l}$ as a function of the magnitude of the uniaxial stress σ. We have performed a numerical calculation by using the following additional approximation: $C_+/C'_+ = (C_-/C'_-)\tilde{1}$ and experimental equilibrium data under hydrostatic conditions and room temperature. To obtain information about the relative concentrations of the moieties of interest in the liquid and solid, we turn to Moynahan *et al*. [29] where small amounts (0.05 mg) of carbonated apatites containing biologically relevant levels of CO_3^{2-} and Na^+ substitutions were placed in solutions of water (10 ml) until equilibrium was reached at approximately 72 h. Ionic concentrations in the liquid were calculated via Inductive Plasma Coupled Optical Emission Spectroscopy. Ionic concentrations in the solid were calculated from quantitative Raman spectroscopy measures of CO_3^{2-} and PO_4^{3-} in the apatites assuming a crystal stoichiometry of $Ca_{9.4}Na_{0.4}(PO_4)_{5.4}(CO_3)_{0.6}(OH)_{1.8}$ as calculated for biomimetic apatites in [17]. These measurements result in:

$\bar{C}_{Ca}^L = 0.532$ mol m^{-3}, $\bar{C}_{Na}^L = 1.755$ mol m^{-3}, $\bar{C}_C^L = 0.010$ mol m^{-3}, $\bar{C}_P^L = 0.331$ mol m^{-3}, $\bar{C}_{Ca}^S = 28\,900$ mol m^{-3}, $\bar{C}_{Na}^s = 3450$ mol m^{-3}, $\bar{C}_C^s = 5500$ mol m^{-3} and $\bar{C}_P^s = 15\,200$ mol m^{-3} with $\bar{V}^S = 1.61 \times 10^{-8}$ m^3 and $L = 1 \times 10^{-5}$ m^3, with this $k_{Ca} = 54\,323$, $k_{Na} = 1966$, $k_C = 550\,000$ and $k_P = 45\,921$.

Wingender *et al*. [18] have shown that Young's modulus of near stoichiometric apatite is $Y \sim 100$ GPa and that it drops by $\Delta Y \sim -50$ GPa for an increase in CO_3^{2-} of ~20 wt% [17,18]. To convert wt% into mol m^{-3}, we use a molecular weight of CO_3^{2-} of 60×10^{-3} kg mole^{-1} and the density of apatite under hydrostatic conditions of 3.17 g cm^{-3}. A 20 wt% change in composition corresponds to approximately 10^4 mole m^{-3}. This enables us to estimate $Z \sim 5 \times 10^{-5}\mathcal{E}$. We also choose the temperature to be $\theta = 300$ K.

In figure 3, we report the relative change in thickness of the solid, measured by the quantity $\Delta l/L - \bar{l}$ as a function of the applied uniaxial stress σ. The stress is varied between 0.5 and 4 GPa. Counterintuitively, the thickness of the solid aggregate increases with increasing stress. Stress induces recrystallization of the solid.

Furthermore, the recrystallization of the apatite is accompanied by a decrease in Ca^{2+} and CO_3^{2-} contents relative to the hydrostatic composition (figure 4). The cation and anion lattice constraints then impose an increase in sodium content as well as an increase in phosphate.

In equation (2.40*a*), since k_{Ca} is greater than k_{Na}, the change Δ'_{Ca} will always vary inversely with the thickness of the apatite solid. For Δ'_C (equation (2.40*b*)), since $k_C - k_P > 0$, the sign of the variation in carbonate composition will depend on the sign and magnitude of $Z/R\theta$. Here, $Z/R\theta$ is negative but too small to change the sign of the variation in carbonate content.

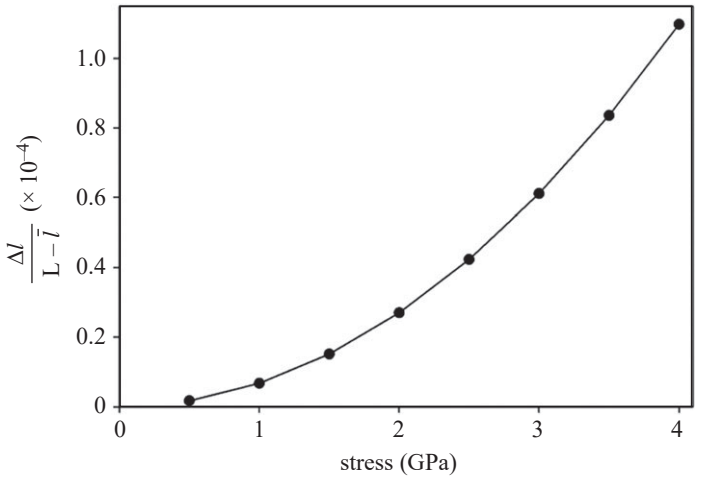

Figure 3. Relative thickness of the solid apatite in equilibrium with an aqueous solution as a function of applied uniaxial stress.

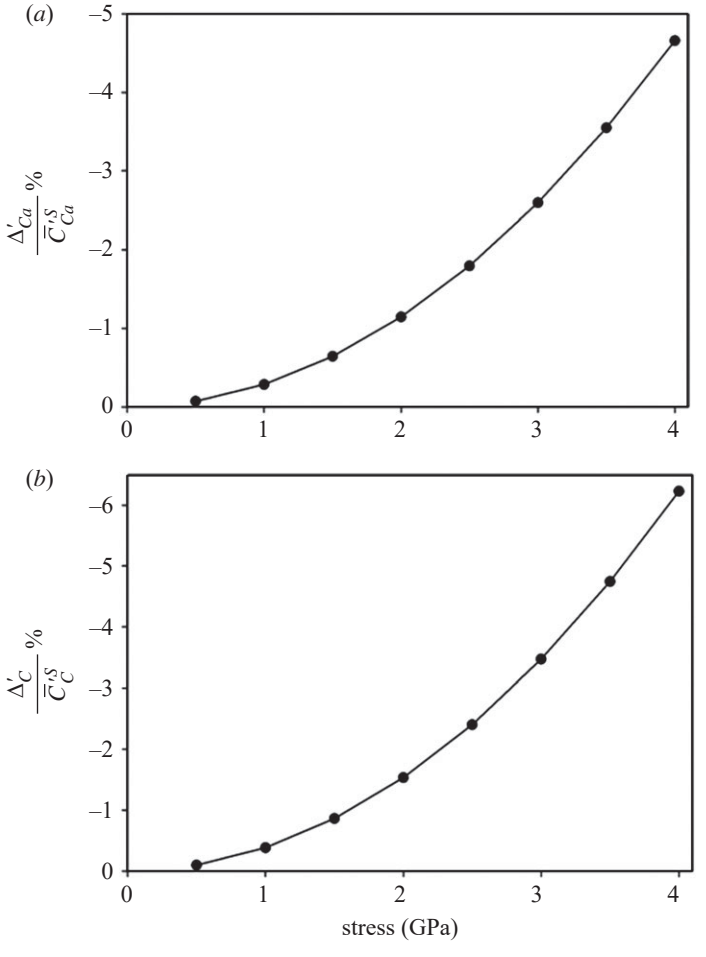

Figure 4. Change in (*a*) calcium and (*b*) carbonate content relative to the hydrostatic equilibrium compositions as functions of stress.

3. Discussion

Results presented in §2e elucidate the effects of applied load on the mineralization of hard tissues such as bone. The recommendation that individuals engage in weight-bearing exercise to promote bone growth and mineralization [30] have mainly centred on the idea of cellular mechanotransduction. Only recently has physiochemical stimulation of mineralization, mostly via increased fluid flow/transport in the collagen matrix, been suggested as a possible benefit of exercise [14,15]. However, the results presented here show another layer of benefit, indicating that applied stress during weight-bearing activities will simultaneously promote mineralization via crystal growth irrespective of cellular and matrix contributions.

In this model, the bone mineral composition is shown to shift towards reduced calcium and carbonate content with applied load. In terms of the classically reported Calcium to Phosphate ratio (Ca/P), this would suggest a decrease in Ca/P with applied stress which has traditionally been used to describe a decrease in mineral maturation [31,32]. Similarly, a drop in the carbonate to phosphate ratio (CO_3^{2-}/PO_4^{3-}) has often been used by bone biologists as an indicator of increased cellular remodelling [33,34]. However, the measurements presented here report these compositional changes in response to applied load irrespective of cellular and maturation behaviours. Therefore, it is important to understand the thermodynamics of bone mineral in stressed environments like bone when considering the meaning or cause of compositional changes.

4. Conclusion

The addition of previously established material simulation techniques, such as DFT and MD, and experimental measurements into our apatite specific model of chemical equilibrium of solids under stress enables the solving of complex biological problems which have until now remained unaddressed. In this work, we examined the dissolution/recrystallization behaviour of biomimetic apatite solids under stress in equilibrium with aqueous solutions. Our study has shown that uniaxial applied stress promotes mineral crystallization. This counterintuitive result points to another mechanism by which load bearing exercise promotes the mineralization of hard tissues, such as bone, thus supporting current medical recommendations to use applied stresses as a means of maintaining bone density with ageing, paralysis and space flight [35–39]. Future work will look to experimentally validate this work as well as examine the synergy between stress and chemical reactions relative to pH in the aqueous solution in controlling mineral dissolution/crystallization.

Data accessibility. This article does not contain any additional data.

Authors' contributions. A.C.D.: conceptualization, data curation, formal analysis, funding acquisition, investigation, methodology, project administration, resources, software, supervision, validation, writing—original draft; P.A.D.: conceptualization, formal analysis, investigation, methodology, supervision, writing—original draft, writing—review and editing; M.L.: conceptualization, investigation, resources, software, visualization, writing—review and editing; K.M.: investigation, validation, writing—review and editing.

All authors gave final approval for publication and agreed to be held accountable for the work performed therein.

Conflict of interest declaration. We declare we have no competing interests.

Funding. A.C.D. was funded by NSF CAREER grant no. 2044870.

Acknowledgements. P.A.D. would like to acknowledge many discussions with F.C. Larché on the topic of thermochemical equilibrium of stressed solids prior to his passing.

References

1. Currey JD. 2002 *Bones: structure and mechanics*. Princeton, NJ: Princeton University Press.
2. Allgrove J, Shaw NJ. 2015 A practical approach to vitamin D deficiency and rickets. *Endocr Dev.* **28**, 119–133. (doi:10.1159/000381000)

3. Currey JD. 1969 The mechanical consequences of variation in the mineral content of bone. *J. Biomech.* **2**, 1–11. (doi:10.1016/0021-9290(69)90036-0)
4. Haba Y, Lindner T, Fritsche A, Schiebenhöfer A-K, Souffrant R, Kluess D, Skripitz R, Mittelmeier W, Bader R. 2012 Relationship between mechanical properties and bone mineral density of human femoral bone retrieved from patients with osteoarthritis. *Open Orthop J* **6**, 458–463. (doi:10.2174/1874325001206010458)
5. Wolff J. 1892 *Das gesetz der transformation der knochen*. Berlin, Germany: Hirschwald.
6. Galilei G. 1990 *Discorsi e dimostrazioni matematiche intorno a due nuove scienze attenenti alla mecanica ed i movimenti locali*. Turin, Italy: Enaudi.
7. Choi JUA, Kijas AW, Lauko J, Rowan AE. 2021 The mechanosensory role of osteocytes and implications for bone health and disease states. *Front. Cell Dev. Biol.* **9**, 770143. (doi:10.3389/fcell.2021.770143)
8. Iandolo D, Strigini M, Guignandon A, Vico L. 2021 Osteocytes and weightlessness. *Curr. Osteoporos Rep.* **19**, 626–636. (doi:10.1007/s11914-021-00713-8)
9. Scott A, Khan KM, Duronio V, Hart DA. 2008 Mechanotransduction in human bone: in vitro cellular physiology that underpins bone changes with exercise. *Sports Med. (Auckland, N.Z.)* **38**, 139–160. (doi:10.2165/00007256-200838020-00004)
10. Jee SS, Thula TT, Gower LB. 2010 Development of bone-like composites via the polymer-induced liquid-precursor (PILP) process. Part 1: Influence of polymer molecular weight. *Acta Biomater.* **6**, 3676–3686. (doi:10.1016/j.actbio.2010.03.036)
11. Wang Y *et al.* 2012 The predominant role of collagen in the nucleation, growth, structure and orientation of bone apatite. *Nat. Mater.* **11**, 724–733. (doi:10.1038/nmat3362)
12. Olszta MJ, Odom DJ, Douglas EP, Gower LB. 2003 A new paradigm for biomineral formation: mineralization via an amorphous liquid-phase precursor. *Connect. Tissue Res.* **44**(Suppl. 1), 326–334. (doi:10.1080/03008200390181852)
13. Kim D, Lee B, Thomopoulos S, Jun YS. 2016 In situ evaluation of calcium phosphate nucleation kinetics and pathways during intra- and extrafibrillar mineralization of collagen matrices. *Cryst. Growth Des.* **16**, 5359–5366. (doi:10.1021/acs.cgd.6b00864)
14. Kim D, Lee B, Marshall B, Thomopoulos S, Jun Y-S. 2021 Cyclic strain enhances the early stage mineral nucleation and the modulus of demineralized bone matrix. *Biomater. Sci.* **9**, 5907–5916. (doi:10.1039/D1BM00884F)
15. Du T, Niu X, Hou S, Xu M, Li Z, Li P, Fan Y. 2020 Highly aligned hierarchical intrafibrillar mineralization of collagen induced by periodic fluid shear stress. *J. Biomed. Mater. Res. B Appl. Biomater.* **8**, 2562–2572. (doi:10.1039/C9TB02643F)
16. Wopenka B, Pasteris JD. 2005 A mineralogical perspective on the apatite in bone. *Mater. Sci. Eng. C* **25**, 131–143. (doi:10.1016/j.msec.2005.01.008)
17. Deymier AC *et al.* 2017 Protein-free formation of bone-like apatite: new insights into the key role of carbonation. *Biomaterials* **127**, 75–88. (doi:10.1016/j.biomaterials.2017.02.029)
18. Wingender B, Azuma M, Krywka C, Zaslansky P, Boyle J, Deymier A. 2021 Carbonate substitution significantly affects the structure and mechanics of carbonated apatites. *Acta Biomater.* **122**, 377–386. (doi:10.1016/j.actbio.2021.01.002)
19. Larché FC, Cahn JW. 1984 The interactions of composition and stress in crystalline solids. *J. Res. Natl Bur Stand (1977)* **89**, 467–500. (doi:10.6028/jres.089.026)
20. Larché F, Cahn JW. 1973 A linear theory of thermochemical equilibrium of solids under stress. *Acta Metall.* **21**, 1051–1063. (doi:10.1016/0001-6160(73)90021-7)
21. Johnson WC, Schmalzried H. 1993 Phenomenological thermodynamic treatment of elastically stressed ionic crystals. *J. Am. Ceram. Soc.* **76**, 1713–1719. (doi:10.1111/j.1151-2916.1993.tb06639.x)
22. De Leeuw NH. 2004 A computer modelling study of the uptake and segregation of fluoride ions at the hydrated hydroxyapatite (0001) surface: introducing a $Ca_{10}(PO_4)_6(OH)_2$ potential model. *Phys. Chem. Chem. Phys.* **6**, 1860. (doi:10.1039/B313242K)
23. Mkhonto D, de Leeuw NH. 2002 A computer modelling study of the effect of water on the surface structure and morphology of fluorapatite: introducing a $Ca_{10}(PO_4)_6F_2$ potential model. *J. Mater. Chem* **12**, 2633–2642. (doi:10.1039/b204111a)
24. Ren F, Lu X, Leng Y. 2013 Ab initio simulation on the crystal structure and elastic properties of carbonated apatite. *J. Mech. Behav. Biomed. Mater.* **26**, 59–67. (doi:10.1016/j.jmbbm.2013.05.030)

25. Peroos S, Du Z, de Leeuw NH. 2006 A computer modelling study of the uptake, structure and distribution of carbonate defects in hydroxy-apatite. *Biomaterials* **27**, 2150–2161. (doi:10.1016/j.biomaterials.2005.09.025)
26. Fast L, Wills JM, Johansson B, Eriksson O. 1995 Elastic constants of hexagonal transition metals: theory. *Phys. Rev. B Condensed Matter* **51**, 17 431–17 438. (doi:10.1103/PhysRevB.51.17431)
27. Menéndez-Proupin E, Cervantes-Rodríguez S, Osorio-Pulgar R, Franco-Cisterna M, Camacho-Montes H, Fuentes ME. 2011 Computer simulation of elastic constants of hydroxyapatite and fluorapatite. *J. Mech. Behav. Biomed. Mater.* **4**, 1011–1020. (doi:10.1016/j.jmbbm.2011.03.001)
28. Ching WY, Rulis P, Misra A. 2009 Ab initio elastic properties and tensile strength of crystalline hydroxyapatite. *Acta Biomater.* **5**, 3067–3075. (doi:10.1016/j.actbio.2009.04.030)
29. Moynahan MM, Wong SL, Deymier AC. 2021 Beyond dissolution: Xerostomia rinses affect composition and structure of biomimetic dental mineral in vitro. *PLoS ONE* **16**, e0250822. (doi:10.1371/journal.pone.0250822)
30. NIH Osteoporosis and Related Bone Diseases National Resource Center. 2018 Exercise for Your Bone Health. Bethesda, MD: National Institute of Health.
31. Eanes ED, Meyer JL. 1977 The maturation of crystalline calcium phosphates in aqueous suspensions at physiologic pH. *Calcified Tissue Res.* **23**, 259–269. (doi:10.1007/BF02012795)
32. Mahamid J, Sharir A, Addadi L, Weiner S. 2008 Amorphous calcium phosphate is a major component of the forming fin bones of zebrafish: indications for an amorphous precursor phase. *Proc. Natl Acad. Sci. USA* **105**, 12 748–12 753. (doi:10.1073/pnas.0803354105)
33. Boskey AL, Imbert L. 2017 Bone quality changes associated with aging and disease: a review. *Ann. N Y Acad. Sci.* **1410**, 93–106. (doi:10.1111/nyas.13572)
34. Boskey AL. 2013 Bone composition: relationship to bone fragility and antiosteoporotic drug effects. *BoneKEy Rep* **2**, 47–58. (doi:10.1038/bonekey.2013.181)
35. Sibonga J *et al.* 2019 Resistive exercise in astronauts on prolonged spaceflights provides partial protection against spaceflight-induced bone loss. *Bone* **128**, 112037. (doi:10.1016/j.bone.2019.07.013)
36. Deymier AC, Schwartz AG, Lim C, Wingender B, Kotiya A, Shen H, Silva MJ, Thomopoulos S. 2020 Multiscale effects of spaceflight on murine tendon and bone. *Bone* **131**, 115152. (doi:10.1016/j.bone.2019.115152)
37. Berg-Johansen B, Liebenberg EC, Li A, Macias BR, Hargens AR, Lotz JC. 2016 Spaceflight-induced bone loss alters failure mode and reduces bending strength in murine spinal segments. *J. Orthop. Res.* **34**, 48–57. (doi:10.1002/jor.23029)
38. Deymier AC, Schwartz AG, Cai Z, Daulton TL, Pasteris JD, Genin GM, Thomopoulos S. 2019 The multiscale structural and mechanical effects of mouse supraspinatus muscle unloading on the mature enthesis. *Acta Biomater.* **83**, 302–313. (doi:10.1016/j.actbio.2018.10.024)
39. Narici MV, Boer MD. 2011 Disuse of the musculo-skeletal system in space and on earth. *Eur. J. Appl. Physiol.* **111**, 403–420. (doi:10.1007/s00421-010-1556-x)